Semileptonic and rare decays at Belle II

D. DORNER* on behalf of the Belle II collaboration
Institute of High Energy Phyiscs
Austrian Academy of Sciences

The Belle II collaboration presents their first measurements of the magnitude of the Cabibbo-Kobayashi-Maskawa matrix elements $|V_{cb}|$ and $|V_{ub}|$, as well as their first branching fraction measurement of $B \to K^*\ell^+\ell^-$ based on up to 189.26 fb^{-1} of data collected at the $\Upsilon(4S)$ resonance. In all presented analyses the hadronic tag from Belle II's full event interpretation was used. $|V_{cb}|$ was measured using $B^0 \to D^{*-}\ell^+\nu_\ell$ by performing a fit to its w distribution. In addition, the results of an inclusive $|V_{cb}|$ fit based on measurements of q^2 moments from Belle II and Belle is presented. $|V_{ub}|$ was obtained using a fit to the q^2 distribution of $B^+ \to \pi^0 e^+\nu_e$ and $B^0 \to \pi^- e^+\nu_e$.

1 Introduction

1.1 Semileptonic and rare decays

In the standard model (SM) of particle physics quark mixing can occur in weak interactions, which is described by the unitary 3×3 Cabibbo-Kobayashi-Maskawa(CKM) matrix. The probability of a flavor change of $b \to c$ or $b \to u$ is proportional to the squared magnitude of the matrix elements $|V_{cb}|^2$ and $|V_{ub}|^2$, respectively.[1]

The unitarity of the CKM matrix in the SM can be probed experimentally, e.g. by measurements of $|V_{cb}|$ and $|V_{ub}|$. Semileptonic decays $B \to X_q\ell\nu$ ($\ell = e, \mu$) can be used for precision measurements of these matrix element magnitudes.

In addition semileptonic and rare decays can be used to search for new physics such as lepton flavor universality (LFU) violation by measuring branching fraction ratios, e.g. $R(D^{(*)}) = \frac{\mathcal{B}(B\to D^{(*)}\tau\nu_\tau)}{\mathcal{B}(B\to D^{(*)}\ell\nu_\ell)}$, which shows a 3σ tension with the SM prediction(fig.1a).

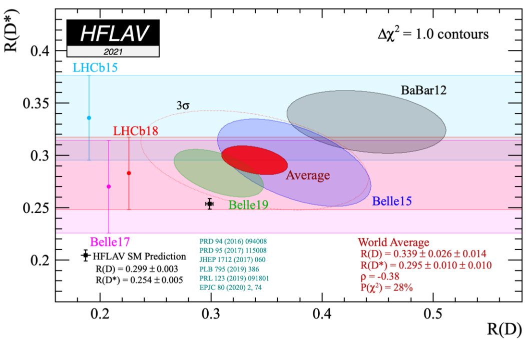

(a) 3σ discrepancy between the measured world average of $R(D^{(*)})$ (red) and the SM prediction (black data point) [2]

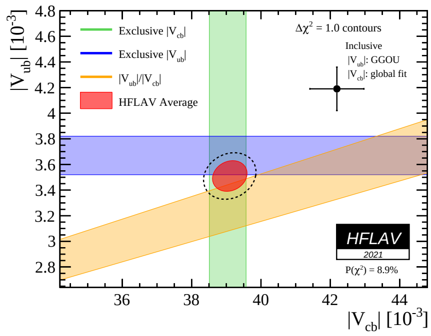

(b) Current 3σ discrepancy between inclusive (black) and exclusive (red) $|V_{cb}|$ and $|V_{ub}|$ measurements [2]

Figure 1: Plots provided by the heavy flavor averaging group (HFLAV [2]) showing the discrepancies of $R(D^{(*)})$ (a) and $|V_{cb}|$ and $|V_{ub}|$ (b)

1.2 Status of $|V_{cb}|$ and $|V_{ub}|$

$|V_{cb}|$ and $|V_{ub}|$ can be measured using two different approaches, namely exclusive and inclusive. In exclusive reconstructions a specific final state is reconstructed, e.g. $B \to D^{(*)}\ell\nu$ or $B \to \pi\ell\nu$. In the inclusive method all final states are reconstructed, e.g. $B \to X_c\ell\nu$ or $B \to X_u\ell\nu$.

The quark currents of semileptonic decays are described using hadronic matrix elements. In exclusive measurements the hadronic matrix elements are parameterized using form factors. Input, e.g. from lattice QCD is required to determine the form factor normalization. In inclusive measurements one uses the heavy quark expansion (HQE).[1] Both methods should agree with each other, however fig.1b shows a long standing 3σ discrepancy between exclusive and inclusive measurements of $|V_{cb}|$ and $|V_{ub}|$.

*E-Mail: daniel.dorner@oeaw.ac.at

2 SuperKEKB and Belle II

2.1 SuperKEKB

The data used for Belle II measurements is produced at the asymmetric e^-e^+ collider SuperKEKB located in Tsukuba, Japan. SuperKEKB collides e^- and e^+ with an energy of 7 GeV and 4 GeV, respectively. This leads to collisions at the $\Upsilon(4S)$ resonance with a center of mass energy of 10.58 GeV. $\Upsilon(4S)$ mesons decay to neutral or charged $B\overline{B}$ pairs with a branching fraction of $\sim 50\%$ for each pair. Clean events with well known initial states are produced due to the collided particles being fundamental.

The design luminosity of SuperKEKB is 6.5×10^{35} cm^{-2}s^{-1}, which is ~ 30 times higher than its predecessor KEKB. The increase in luminosity is achieved by using the nanobeam scheme (20$\times$smaller beam spot) and higher beam currents[3]. While the design luminosity has not yet been reached the collider holds the current luminosity world record of $\sim 4 \times 10^{34}$ cm^{-2}s^{-1}.

So far SuperKEKB delivered 428fb^{-1} of data and the results presented use a data set of up to 189.3 fb^{-1}. Starting in July 2022 a long shutdown will start in order to to upgrade detector components, which will last until fall 2023. The obtained data up until that shutdown are shown in the luminosity estimation in fig.2a.

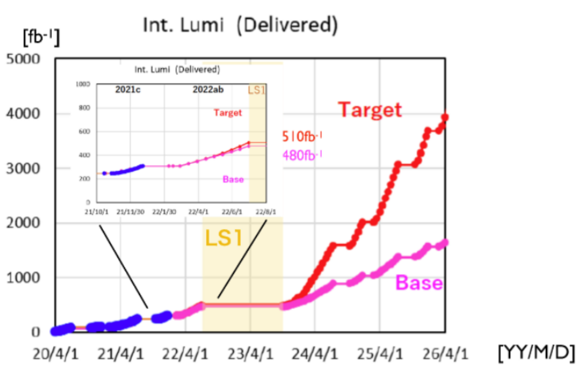

(a) Target luminosity(red) and conservatively estimated luminosity(magenta) until the start of the long shutdown(LS1) and a post LS1 prediction up to 2026 [4]

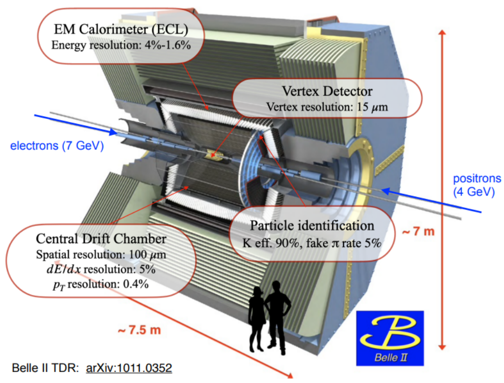

(b) Illustration of the Belle II detector [3]

Figure 2: The estimated luminosity until the shut down (a) and the Belle II detector (b)

2.2 Belle II

The measuring of the momenta, tracks and energies of the final state particles resulting from the collisions and their identification is done by the Belle II detector, shown in fig.2b. Belle II is a hermetic detector resulting in a high solid angle coverage.

An important feature of the detector is its good particle identification capability. Belle II's muon identification efficiency of 88% is already superior to its predecessor. The electron identification efficiency of 86% (see fig.3a) is not yet superior to Belle, but steadily improving[5].

In addition, the detector has a high gamma detection efficiency[6], as shown in fig.3b. This is needed for the reconstruction of neutral particle, e.g. π^0, which is important for the reconstruction of decay modes like $K^{*+} \to K^+\pi^0$.

2.3 Tag-side reconstruction

Due to the previously described features of the experimental setup, decays can be reconstructed either untagged or tagged using Belle II's full event interpretation[7]. In the untagged approach only the signal-side B meson B_{sig} is reconstructed, while in the tagged approach the B_{sig} meson as well as the so-called tag-side B meson B_{tag} are reconstructed.

Using the tagged reconstruction one can infer the flavor of B_{sig}, e.g. $\bar{B}^0_{tag} \to B^0_{sig}$, and fully resolve event kinematics by fully reconstructing the second B meson in the $\Upsilon(4S)$ event, e.g. $p_\nu = p_{e^+e^-} - p_\ell - p_{B_{tag}} - p_{X_c}$.

The downside of tagging is its efficiency. In the hadronic tag $\mathcal{O}(10,000)$ decay chains are reconstructed with an overall efficiency of $\mathcal{O}(0.1)\%$, therefore losing a substantial amount of events. While the efficiency of the hadronic tag is still in the sub-percent it is increased by 30-50% in comparison to Belle at the same purity.

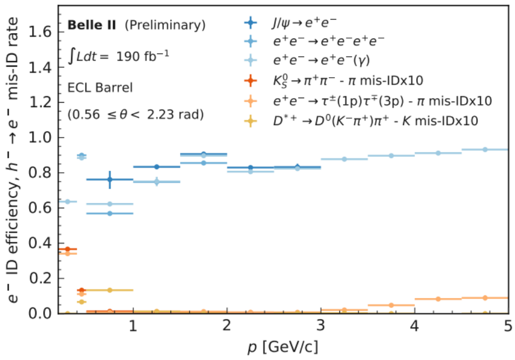

(a) e identification efficiency(blue) and mis-identification rate(orange) originating from different decays as a function of the e-momentum [5]

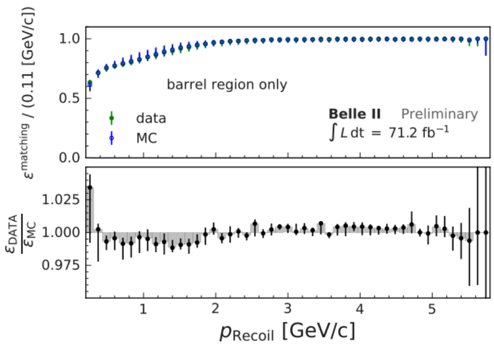

(b) The upper plot shows Belle II's efficiency of matching a photon to an ECL cluster resulting from p_{Recoil}. The lower plot compares data and MC efficiencies. [6]

Figure 3: Belle II's current e-identification (a) and photon reconstruction (b) capabilities

3 Semileptonic decays

3.1 Determination of $|V_{ub}|$ from $B \to \pi e\nu$

$|V_{ub}|$ was measured by reconstructing $B^+ \to \pi^0 e^+ \nu_e$ and $B^0 \to \pi^- e^+ \nu_e$ using the hadronic tag. The main challenge of this analysis is its small sample size, due to the inherently low branching fraction of the decay and the π^0 reconstruction.

The signal yield was obtained using a likelihood-fit to the missing mass squared $M_{miss}^2 = (p^*_{e^+e^-} - p^*_{B_{tag}} - p^*_e - p^*_\pi)^2$ in three bins of the momentum transfer squared $q^2 = (p^*_{e^+e^-} - p^*_{B_{tag}} - p^*_\pi)^2$, where * denotes the center of mass frame.

These yields are unfolded and used to determine $|V_{ub}|$ using its relation to the differential branching fraction

$$\frac{d\mathcal{B}(B \to \pi e\nu)}{dq^2} \propto |V_{ub}|^2 f_+^2(q^2) \tag{1}$$

$|V_{ub}|$ was obtained by performing a combined χ^2-fit to $\frac{d\mathcal{B}}{dq^2}$ using BCL parameters[8] and LQCD constraints[9]. The resulting fit, shown in fig.4, yielded $|V_{ub}| = (3.88 \pm 0.45) \times 10^{-3}$. The uncertainty includes both statistical and systematic uncertainties. Simultaneously the branching fractions over all bins of q^2 of the individual channels were measured to be $\mathcal{B}(B^0 \to \pi^- e^+ \nu_e) = (1.43 \pm 0.27_{stat} \pm 0.07_{sys}) \times 10^{-4}$ and $\mathcal{B}(B^+ \to \pi^0 e^+ \nu_e) = (8.33 \pm 1.67_{stat} \pm 0.55_{sys}) \times 10^{-5}$ [10].

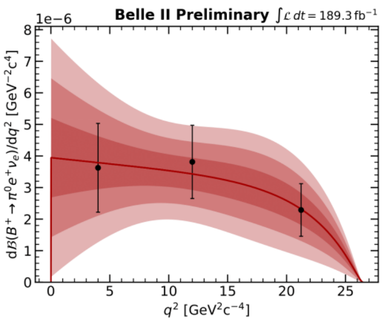

(a) $B^+ \to \pi^0 e^+ \nu_e$

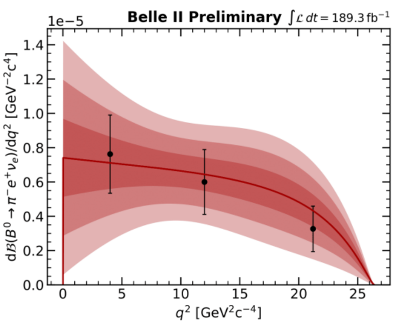

(b) $B^0 \to \pi^- e^+ \nu_e$

Figure 4: The combined χ^2-fit projection of $\frac{d\mathcal{B}}{dq^2}$ to the B^+(a) and B^0(b) decays [10]

3.2 Determination of $|V_{cb}|$ from $B \to D^* \ell\nu$

The decay $B^0 \to D^{*-} \ell^+ \nu_\ell$ was reconstructed with the subsequent decays $D^{*-} \to \bar{D}^0 \pi_S^-$ and $\bar{D}^0 \to K^+ \pi^-$ using the hadronic tag. Here π_S denotes the slow pion with a momentum below 300 MeV.

$|V_{cb}|$ can be extracted from $B^0 \to D^{*-}\ell^+\nu_\ell$ by using the relation

$$\frac{d\Gamma(\mathcal{B}(B \to D^*\ell\nu_\ell))}{dw} \propto \eta_{EW}^2 F^2(w)|V_{cb}|^2 \tag{2}$$

where w is the hadronic recoil $w = \frac{P_B \cdot P_{D^*}}{m_B m_D} = \frac{m_B^2 + m_{D*} - q^2}{2m_B m_{D^*}}$. In this analysis the product $\eta_{EW}F(1)|V_{cb}|$ was measured using the CLN parameterization[11], where $F(w)$ is parameterized using ρ^2, $R_1(1)$ and $R_2(1)$. ρ^2 was determined by the fit, while an external input[2] was used for $R_1(1)$ and $R_2(1)$.

The result of a χ^2-fit to the differential branching fraction $\frac{d\Gamma}{dw}$ in ten bins of the unfolded w distribution is shown in fig.5a. Fig.5b shows the result of the χ^2 function in the plane of $\eta_{EW}F(1)|V_{cb}|$ and ρ^2. This analysis measured $\eta_{EW}F(1)|V_{cb}| = (34.6 \pm 2.5) \times 10^{-3}$ and $\rho^2 = 0.94 \pm 0.21$ yielding $|V_{cb}| = (37.9 \pm 2.7) \times 10^{-3}$ by using the external inputs $\eta_{EW} = 1.0066$[12] and $F(1) = 0.906 \pm 0.004_{stat} \pm 0.0012_{sys}$[12]. At the same time the analysis obtained the branching fraction $\mathcal{B}(B \to D^*\ell\nu) = (5.27 \pm 0.22_{stat} \pm 0.38_{sys})\%$ over the whole w spectrum, with the uncertainty being systematically dominated by the uncertainty in the π_S efficiency.

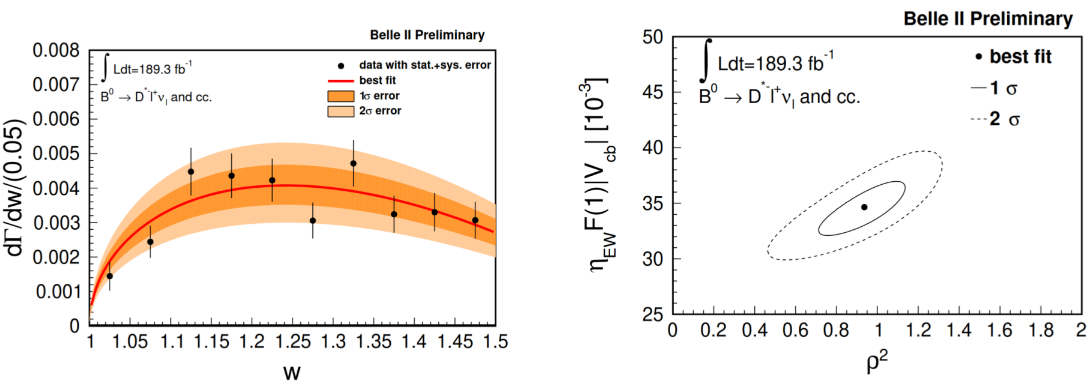

(a) Fit projection to $\frac{d\Gamma}{dw}$ in ten bins of w

(b) Result of the χ^2-fit in the plane of $\eta_{EW}F(1)|V_{cb}|$ and ρ^2

Figure 5: Results of the χ^2-fit to $\frac{d\Gamma}{dw}$ obtained from $B \to D^*\ell\nu$

3.3 Determination of $|V_{cb}|$ from $B \to X_c\ell\nu$

$|V_{cb}|$ can be determined with an inclusive analysis by describing the decay width with the operator product expansion(OPE): $\Gamma = \frac{G_F^2 m_b^5}{192\pi^3}|V_{cb}|^2(1 + \frac{c_5(\mu)O_5(\mu)}{m_b^2} + \mathcal{O}(\frac{1}{m_b^3}) + \mathcal{O}(\frac{1}{m_b^4}) + ...)$, where O_i are non-perturbative hadronic matrix elements, c_i perturbative coefficients and m_b the b quark mass.

In the established approach the moments of the lepton energy E_ℓ and the hadronic mass M_X are used to determine the parameters of the expansion[13]. However the number of parameters rises quickly at higher orders making a truncation of the series at the third element necessary leading to a precision loss.

This analysis measured the q^2 moments used in a novel approach[14], where the proliferation of parameters is avoided by exploiting the reparameterization invariance. This invariance does not apply to all observables, but holds for q^2 moments. By determining the q^2 moments one can go up to the order of n = 4 instead of n = 3.

The moments are determined using the relation

$$\langle q^{2n} \rangle = \frac{\sum_i w_i(q^2) q^{2n}_{i,calib}}{\sum_i w_i(q^2)} \cdot \mathcal{C}_{calib} \cdot \mathcal{C}_{gen} \tag{3}$$

An event-wise signal probability $w(q^2)$ can be calculated using a background normalisation determined by a fit to M_X. The reconstructed $(q^{2n})_{reco}$ needs to be calibrated to account for resolution and detector effects leading to $(q^{2n})_{calib}$ and in addition, a correction to $\mathcal{C}_{calib}$ is multiplied to take calibration biases into consideration. To correct for selection effects $\mathcal{C}_{gen}$ is multiplied [15][16].

However, while the $\langle q^{2n} \rangle$ were measured by the Belle II collaboration, a fit to these moments was done independently by F. Bernlochner et.al.[17]. This fit was done for $\langle q^{2n} \rangle$ obtained from Belle II data, from Belle data[15] and also by combining the measurements of both analyses. Using the semileptonic branching fraction $\mathcal{B}(B \to X_c\ell\nu_\ell) = (10.63 \pm 0.19)\%$ this method resulted in $|V_{cb}| = (41.69 \pm 0.63) \times 10^{-3}$[17]. The fit-projection to the measured q^2 moments for the combined fit is shown in fig.6.

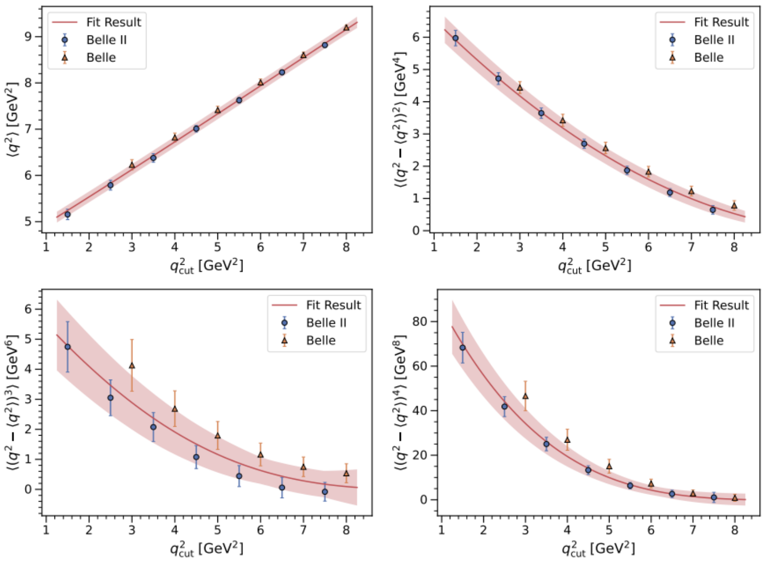

Figure 6: Fit-projection of the combined fit to the distribution of the q^2 moments up to $n = 4$. The blue data points represent the Belle II measurements and the orange data points the Belle measurements, including their respective uncertainties.[17]

4 Rare decays

4.1 Determination of the $B \to K^*\ell\ell$ branching fraction

Quark flavor transitions $b \to s$ are forbidden at the tree level in the SM, therefore $B \to K^{(*)}\ell\ell$ decays can be used to probe for new physics effects, which enhance or suppress the branching ratios. Recent measurements of the ratio $R(K^{(*)}) = \frac{\mathcal{B}(B\to K^{(*)}\mu^+\mu^-)}{\mathcal{B}(B\to K^{(*)}e^+e^-)}$ at LHCb showed a 3.1σ deviation from the SM prediction[18][19][20].

At Belle II the branching fraction of $B \to K^*\ell\ell$ was measured by reconstructing the subsequent decays $K^* \to K^+\pi^-, K^+\pi^0, K^0_s\pi^+$ using the hadronic tag and excluding the J/ψ and $\psi(2S)$ resonances[21].

A 2D likelihood-fit to the beam constrained mass $M_{bc} = \sqrt{s/4 - p_B^{*2}}$ and the energy deviation of the reconstructed B meson from half the beam energy in the center of mass frame $\Delta E = E_B^* - \sqrt{s}/2$ is used to extract the signal yield. Fig.7 shows the resulting fit-projections to the distributions of M_{bc} and ΔE.

The branching fraction was measured over the whole q^2 range with a signal significance of $3.6\sigma - 5.9\sigma$. The results of the μ-mode, e-mode and the combined fraction of both modes were measured to be $\mathcal{B}(B \to K^*\mu\mu) = (1.28 \pm 0.29^{+0.08}_{-0.07}) \times 10^{-6}$, $\mathcal{B}(B \to K^*ee) = (1.04 \pm 0.48^{+0.09}_{-0.09}) \times 10^{-6}$ and $\mathcal{B}(B \to K^*\ell\ell) = (1.22 \pm 0.28^{+0.08}_{-0.07}) \times 10^{-6}$.[21] The first uncertainty being statistical and the second systematical[21].

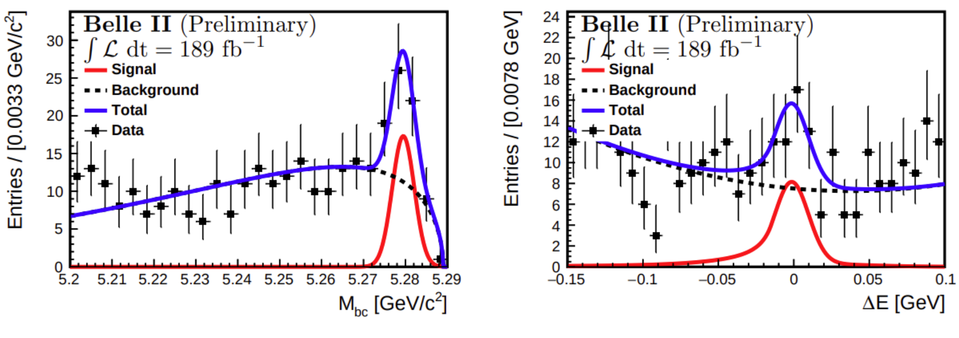

Figure 7: Post-fit distributions of M_{bc}(left) and ΔE(right) for $B \to K^*\ell\ell$. With the red line being the signal shape, the blue line the shape including both background and signal candidates and the dotted black line represents the background distribution[21]

5 Conlcusion

A value of $|V_{cb}| = (37.9 \pm 2.7) \times 10^{-3}$ was obtained from $B^0 \to D^{*-}\ell^+\nu_\ell$ decays in tagged Belle II events. By combining $B^+ \to \pi^0 e^+\nu_e$ and $B^0 \to \pi^- e^+\nu_e$ decays $|V_{ub}| = (3.88\pm0.45)\times10^{-3}$ was measured. The uncertainties on the $|V_{cb}|$ and $|V_{ub}|$ values include both the statistical and systematic uncertainties. An inclusive $|V_{cb}|$ fit by F. Bernlochner et.al.[17] to combined q^2 moments measurements of $B \to X_c \ell \nu$ from Belle and Belle II yielded $|V_{cb}| = (41.69 \pm 0.63) \times 10^{-3}$. In addition, the branching fraction of the rare decay $B \to K^* \ell\ell$ was measured for the first time at Belle II. This analysis yielded a branching fraction of $\mathcal{B}(B \to K^* \ell\ell) = (1.22 \pm 0.28^{+0.08}_{-0.07}) \times 10^{-6}$, where the first uncertainty is statistical and the second systematic.

References

[1] A. J. Bevan et al. "The Physics of the B Factories". In: *The European Physical Journal C* 74.11 (Nov. 2014). ISSN: 1434-6052. DOI: **10.1140/epjc/s10052-014-3026-9**.

[2] Y. Amhis et al. "Averages of b-hadron, c-hadron, and τ-lepton properties as of 2018". In: *The European Physical Journal C* 81.3 (Mar. 2021). DOI: **10.1140/epjc/s10052-020-8156-7**.

[3] T. Abe et al. "Belle II Technical Design Report". In: (2010). DOI: **10.48550/ARXIV.1011.0352**.

[4] The Belle II Collaboration. *Belle II Luminosity*. URL: **https://confluence.desy.de/display/BI/Belle+II+Luminosity** (visited on Aug. 2, 2022).

[5] Charged PID Group and The Belle II Collaboration. "Muon and electron identification efficiencies and hadron-lepton mis-identification rates at Belle II for Moriond 2022". In: (Mar. 2022). URL: **https://docs.belle2.org/record/2895**.

[6] Henrikas Svidras et al. "Measurement of the data to MC ratio of photon reconstruction efficiency of the Belle II calorimeter using radiative muon pair events". In: (Sept. 2021). URL: **https://docs.belle2.org/record/2604/**.

[7] T. Keck, F. Abudinén, et al. "The Full Event Interpretation". In: *Computing and Software for Big Science* 3.1 (Feb. 2019). DOI: **10.1007/s41781-019-0021-8**.

[8] Claude Bourrely, Laurent Lellouch, and Irinel Caprini. "Model-independent description of $B \to \pi l \nu$ decays and a determination of $|V_{ub}|$". In: *Phys. Rev. D* 79 (1 Jan. 2009), p. 013008. DOI: **10.1103/PhysRevD.79.013008**.

[9] A. Bailey et al. "$|V_{ub}|$ from $B \to \pi \ell \nu$ decays and (2+1)-flavor lattice QCD". In: *Physical Review D* 92.1 (July 2015). DOI: **10.1103/physrevd.92.014024**.

[10] Belle II Collaboration et al. "Study of Exclusive $B \to \pi e^+ \nu_e$ Decays with Hadronic Full-event-interpretation Tagging in 189.3 fb^{-1} of Belle II Data". In: (2022). DOI: **10.48550/ARXIV.2206.08102**.

[11] Irinel Caprini, Laurent Lellouch, and Matthias Neubert. "Dispersive bounds on the shape of form factors". In: *Nuclear Physics B* 530.1-2 (Oct. 1998), pp. 153–181. DOI: **10.1016/s0550-3213(98)00350-2**.

[12] Jon A. Bailey et al. "Update of $|V_{cb}|$ from the $\bar{B} \to D^* \ell \bar{\nu}$ form factor at zero recoil with three-flavor lattice QCD". In: *Physical Review D* 89.11 (June 2014). DOI: **10.1103/physrevd.89.114504**.

[13] Andrea Alberti et al. "Precision Determination of the Cabibbo-Kobayashi-Maskawa Element V_{cb}". In: *Physical Review Letters* 114.6 (Feb. 2015). DOI: **10.1103/physrevlett.114.061802**.

[14] Matteo Fael, Thomas Mannel, and K. Keri Vos. "V_{cb} determination from inclusive $b \to c$ decays: an alternative method". In: *Journal of High Energy Physics* 2019.2 (Feb. 2019). DOI: **10.1007/jhep02(2019)177**.

[15] Belle Collaboration et al. "Measurements of q^2 Moments of Inclusive $B \to X_c \ell^+ \nu_\ell$ Decays with Hadronic Tagging". In: (2021). DOI: **10.48550/ARXIV.2109.01685**.

[16] Belle II Collaboration. "Measurement of Lepton Mass Squared Moments in $B \to X_c \ell \bar{\nu}_\ell$ Decays with the Belle II Experiment". In: (2022). DOI: **10.48550/ARXIV.2205.06372**.

[17] Florian Bernlochner et al. "First extraction of inclusive V_{cb} from q^2 moments". In: (2022). DOI: **10.48550/ARXIV.2205.10274**.

[18] Bernat Capdevila et al. "Patterns of New Physics in $b \to s \ell^+ \ell^-$ transitions in the light of recent data". In: *Journal of High Energy Physics* 2018.1 (Jan. 2018). DOI: **10.1007/jhep01(2018)093**.

[19] LHCb Collaboration et al. "Test of lepton universality in beauty-quark decays". In: (2021). DOI: **10.48550/ARXIV.2103.11769**.

[20] R. Aaij, A. S. W. Abdelmotteleb, C. Abellán Beteta, et al. "Tests of Lepton Universality Using $B^0 \to K^0_S \ell^+ \ell^-$ and $B^+ \to K^{*+} \ell^+ \ell^-$ Decays". In: *Physical Review Letters* 128.19 (May 2022). DOI: **10.1103/physrevlett.128.191802**.

[21] Belle II Collaboration et al. "Measurement of branching fraction for $B \to K^* \ell\ell$ at Belle II". In: (Mar. 2022). URL: **https://arxiv.org/abs/2206.05946**.